Chemistry Today

2026, Vol. 02 Issue 01
21-26

Research Article

Analysis of Phosphate (PO_4^{3-}) and Total Iron (Fe) Concentrations in the Main Cooling Water System of Keramasan Combined-Cycle Power Plant

Dinar Adelia[1*], Ade Oktasari[2]

[1,2]*Department of Chemistry, Raden Fatah State Islamic University Palembang, Palembang, Indonesia*

ARTICLE INFORMATION

Received: August 18, 2026
Revised: October 28, 2026
Accepted: October 29, 2026
Available online: November 1, 2026

CORRESPONDENCE

E-mail: dinaaradelia@gmail.com

DOI
https://doi.org/10.68712/zpvssq65

A B S T R A C T

Maintaining water chemistry in cooling circuits is critical for controlling mineral scaling and electrochemical corrosion in power generation systems. This study evaluated the residual concentrations of phosphate (PO_4^{3-}) and total iron (Fe) in the open-recirculating Main Cooling Water (MCW) system at Keramasan Combined-Cycle Power Plant (CCPP), Palembang, South Sumatra. Water samples were monitored spectrophotometrically across 10 monitoring days between January 20 and February 6, 2025. Phosphate levels were quantified via the ascorbic acid-molybdenum blue method, while total iron was determined using the 1,10-phenanthroline method. The analytical results showed that phosphate concentrations ranged from 0.28 to 2.82 mg/L, remaining consistently below the established operational threshold of 6.0-11.0 mg/L. A pronounced decrease in phosphate was observed following the temporary cessation of corrosion inhibitor dosing and concurrent system blowdown during plant maintenance. Conversely, total iron concentrations fluctuated between 0.02 and 0.32 mg/L, successfully complying with the maximum permissible quality standard (< 2.0 mg/L). The sub-optimal phosphate levels indicate an insufficient passivation barrier against metallic corrosion, emphasizing the need to optimize chemical injection dosage and conduct routine upstream monitoring of raw river water to preserve system integrity and thermal efficiency.

Keywords: *Main Cooling Water, Phosphate Concentration, Total Iron, Combined-Cycle Power Plant, Spectrophotometry UV-Vis*

1. Introduction

A Combined-Cycle Power Plant (CCPP) relies on the integration of gas and steam turbine cycles to generate electrical energy efficiently (Fakhry et al., 2024). The continuous and reliable baseload operation of a CCPP depends heavily on water quality, as water serves as the primary working fluid in the steam cycle and acts as an effective heat transfer medium (Rayadi, 2015). The cooling water system plays a vital role in dissipating excess heat from critical plant components. Cooling systems in CCPPs typically comprise two configurations, a Closed Cycle Cooling Water (CCCW) system using demineralized water in a closed loop, and an open-recirculating Main Cooling Water (MCW) system that utilizes external water sources, such as rivers or seas (Dharma, 2018). The MCW infrastructure consists of essential heat-transfer equipment, including circulating water pumps, piping networks, cooling towers, and surface condensers (Muammar et al., 2022).

Maintaining optimal chemical parameters in the MCW is crucial to ensure high heat-transfer efficiency and prevent equipment degradation. Two key chemical parameters requiring stringent monitoring are phosphate (PO_4^{3-}) and total iron (Fe). Phosphate-based chemicals are commonly dosed as corrosion and scale inhibitors to establish a protective passivation layer on metal surfaces. However, excessive phosphate concentrations can induce orthophosphate or calcium phosphate precipitation, leading to scale formation. Scale deposits significantly impair heat transfer, increase pumping energy consumption, and induce localized overheating (Rahmawati et al., 2024).

Conversely, total iron (Fe) in the cooling circuit originates from both the untreated raw water intake and the active electrochemical degradation of carbon steel and metallic alloy components within the system (Syafika et al., 2022). High iron levels indicate ongoing corrosion, particularly across condenser tubes, pump impellers, and cooling tower structures. Severe condenser tube corrosion poses a substantial operational risk,

This is an open-access article distributed under the terms of the Creative Commons Attribution-NonCommercial-ShareAlike 4.0 International.

as tube leaks allow low-purity cooling water to contaminate the high-purity steam cycle feedwater. In addition, iron levels can indicate that metal degradation is occurring in the cooling system, resulting in increased energy consumption and a shorter service life for pipes and pumps, which directly impacts operating costs.

Therefore, in the cooling system at Keramasan Combined-Cycle Power Plant, routine monitoring of phosphate and iron levels is essential to assess inhibitor efficacy and mitigate corrosion rates. This study aims to analyze the levels of phosphate (PO_4^{3-}) and iron (Fe) residues in the main cooling water system at the Keramasan combined-cycle power plant, in order to evaluate the effectiveness of inhibitor injection and its compliance with applicable operational quality standards.

2. Methods

2.1 Sampling Location and Pre-Treatment Context

Water samples were collected from the open-recirculating Main Cooling Water (MCW) system at Keramasan Combined-Cycle Power Plant (CCPP) Palembang, South Sumatra. The plant utilizes raw water abstracted from the Keramasan River, which undergoes pre-treatment in the Water Treatment Plant 2 (WTP 2) facility. The pre-treatment involves chemical coagulation and flocculation using Poly Aluminum Chloride (PAC), sodium hydroxide (NaOH), and organic polymers in a sedimentation basin, followed by clarification through an inclined plate clarifier before entering the cooling tower circuit. In routine WTP 2 operations, effluent make-up water quality is rountinely monitored for turbidity and conductivity to assses clarification efficiency, whereas daily spectrophotometric iron monitoring is exclusively conducted on the active recirculating MCW loop. Sampling was carried out twice daily (at 09:00 and 15:00 WIB) from the cooling tower outlet stream across 10 monitoring days between January 20 and February 6, 2025. The reported daily values were calculated as the arithmetic mean of the two measurement sessions (09:00 and 15:00 WIB) and are expressed as Mean ± Standard Deviation (± SD) to represent analytical reproducibility.

2.2 Materials and Instrumentation

The analytical instruments utilized in this study included a Hach DR 2800 UV-Visible Spectrophotometer, 10 mL matched square quartz/glass cuvettes, 50 mL Erlenmeyer flasks, and precision graduated cylinders. Analytical reagents consisted of PhosVer 3 Phosphate Reagent powder pillows (Hach Method 8048) and FerroVer Iron Reagent powder pillows (Hach Method 8008). Deionized water and untreated sample aliquots were used for reagent preparation and spectrophotometric zeroing.

2.3 Determination of Phosphate (PO_4^{3-}) Concentration

Phosphate concentration was quantified via the ascorbic acid/molybdenum blue method (Method 8048). A 10 mL sample aliquot was measured into a 50 mL Erlenmeyer flask, and the contents of one PhosVer 3 reagent packet were added. The mixture was swirled vigorously for 30 seconds to dissolve the reagent completely and allowed to stand for a 2-minute reaction period to form the blue complex. An unreacted 10 mL sample aliquot was placed in a cuvette to zero the spectrophotometer. Absorbance was subsequently measured at a maximum wavelength (λ_{max}) of 880 nm using the UV-Visible spectrophotometer, and the phosphate concentration was recorded in mg/L.

2.4 Determination of Total Iron (Fe) Concentration

Total iron concentration was evaluated using the 1,10-phenanthroline method (Method 8008). A 10 mL sample aliquot was introduced into a 50 mL Erlenmeyer flask and reacted with one packet of FerroVer reagent. The solution was homogenized for 30 seconds and left undisturbed for 2 minutes to allow complete reduction and complexation, yielding an orange-red tris complex. Following baseline calibration with an untreated sample blank, the absorbance was measured at a wavelength (λ_{max}) of 510 nm on the UV-Visible spectrophotometer, with results reported directly in mg/L.

3. Results and Discussion

3.1 Spectrophotometric Complexation Mechanisms

The determination of phosphate (PO_4^{3-}) and total iron (Fe) concentrations in the main cooling water (MCW) system was performed using a UV-Vis spectrophotometer based on the reaction that forms specific-colored complexes. In the phosphate analysis, PhosVer 3 Phosphate Reagent which comes in the form of white crystalline granules is used. This method, known as the ascorbic acid-molybdate blue method, involves a

 https://doi.org/10.68712/zpvssq65

reaction between orthophosphate ions and ammonium molybdate in an acidic environment, producing a phosphomolybdate complex that upon reduction forms a deep blue color whose intensity is proportional to the phosphate concentration in the sample (λ_{max} = 880 nm). The reaction that occurs is as follows (Anjarsari & Sugiarso, 2019):

$$PO_4^{3-} + 12MoO_4^{2-} + 27H^+ \rightarrow H_3[P(Mo_3O_{10})_4]^{2-} + 12H_2O$$
$$H_3[P(Mo_3O_{10})_4]^{2-} + 2H^+ \rightarrow H_5[P(Mo_3O_{10})_4]$$

For iron determination, the FerroVer reagent, a white powder with a pungent odor reduces all available ferric (Fe^{3+}) and ferrous (Fe^{2+}) species into free ferrous ions, which subsequently coordinate with three 1,10-phenanthroline ligands form a stable orange-red complex $[Fe(C_{12}H_8N_2)_3]^{2+}$ which was measured at λ_{max} = 510 nm as shown in the reaction below (Anjarsari & Sugiarso, 2019):

$$Fe^{2+}_{(aq)} + 3C_{12}H_8N_{2(aq)} \rightarrow [Fe(C_{12}H_8N_2)_3]^{2+}_{(aq)}$$

The analytical monitoring data for the MCW system across the 10 sampling dates at Keramasan Combined-Cycle Power Plant are presented in Table 1.

Table 1. Phosphate (PO_4^{3-}), total iron (Fe), and pH values (Mean ± SD) in the MCW system at Keramasan CCPP

No	Date	PO_4^{3-} (mg/L)	Fe (mg/L)	pH (Mean)
1	20 Jan 2025	2.54 ± 0.18	0.02 ± 0.000	7.95 ± 1.20
2	21 Jan 2025	2.82 ± 0.02	0.02 ± 0.007	6.90 ± 0.14
3	22 Jan 2025	2.55 ± 0.13	0.04 ± 0.035	6.30 ± 0.00
4	23 Jan 2025	2.32 ± 0.13	0.05 ± 0.035	6.10 ± 0.42
5	24 Jan 2025	2.43 ± 0.04	0.11 ± 0.007	6.60 ± 0.42
6	30 Jan 2025	0.92 ± 0.02	0.32 ± 0.389	6.25 ± 0.07
7	31 Jan 2025	0.80 ± 0.04	0.13 ± 0.007	6.85 ± 0.49
8	03 Feb 2025	0.42 ± 0.03	0.08 ± 0.007	7.15 ± 0.21
9	04 Feb 2025	0.28 ± 0.04	0.10 ± 0.014	7.00 ± 0.00
10	06 Feb 2025	0.27 ± 0.04	0.13 ± 0.014	6.05 ± 0.07
Operational Standards		6.0 – 11.0	< 2.0	6.5 – 8.5

3.2 Phosphate Concentration and Inhibitor Depletion

As illustrated in Figure 1, the phosphate concentration demonstrated two distinct operational regimes. From January 20 to January 24, 2025, phosphate levels remained relatively stable within a narrow range of 2.3-2.82 mg/L, reaching a maximum of 2.82 mg/L on January 21. However, a sharp downward trend commenced on January 30 (0.92 mg/L), eventually reaching a minimum of 0.28 mg/L on February 4, 2025.

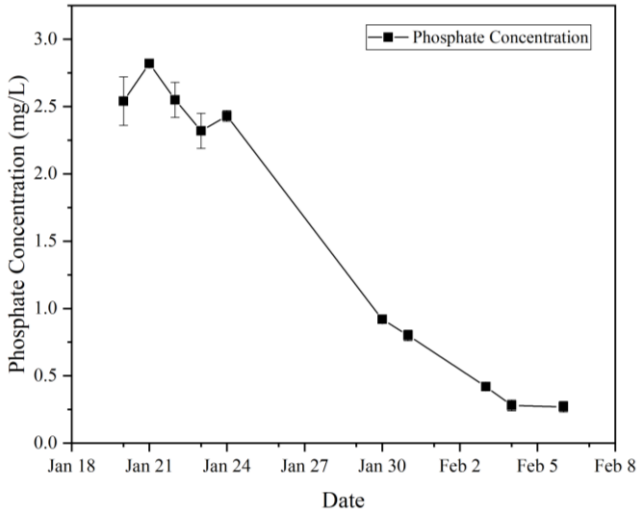


Figure 1. Fluctuation profile of phosphate concentration in the MCW system

This steep decline was directly linked to plant maintenance activities. On January 30-31, chemical injection of corrosion inhibitors was suspended due to condenser inspections. Concurrently, partial cooling tower shutdown for filler replacement that is no longer serviceable and associated system blowdown were performed. This causes uneven phosphate distribution and removes phosphate residues that were previously attached to the cooling tower components. System blowdown discharged phosphate-laden recirculating water, which was subsequently replaced with make-up water containing a lower phosphate level.

Phosphate-based compounds act as anodic corrosion inhibitors by forming an insoluble ferric-phosphate passivation barrier on metal surfaces (Bastidas et al., 2021). Throughout the monitoring period, phosphate levels consistently fell below the plant's operational standard of 6.0-11.0 mg/L. While excessive phosphate (> 11.0 mg/L) risks calcium phosphate scale precipitation and thermal fouling, inadequate phosphate (< 6.0 mg/L) leaves metallic surfaces vulnerable to accelerated electrochemical attack. Furthermore, phosphate ion speciation and the precipitation kinetics of calcium phosphate ($Ca_3(PO_4)_2$) are strongly governed by solution pH and system alkalinity. During the monitoring period, the MCW operating pH was maintained within a neutral to slightly alkaline regime (pH 6.05-7.95, with an average of 6.71 ± 0.58). Under these pH conditions, the primary phosphate species exists predominantly as HPO_4^{2-} and $H_2PO_4^-$, minimizing the thermodynamic drive for spontaneous calcium phospate scaling, with typically requires highly alkaline environments (pH > 8.5) (Demadis & Ketsetzi, 2007). This confirms that the sharp depletion of residual phosphate following January 30 was predominanly attributed to physical dilution via systemic blowdown and the temporary cessation of inhibitor injection, rather than precipitation within the cooling circuit. According to Aprilia & Hardjono, (2023), if the phosphate concentration in the cooling water falls below the threshold, the chemical injection rate must be increased.

3.3 Total Iron Variations and Corrosion Behavior

As depicted in Figure 2, total iron concentrations fluctuated within the range of 0.02 to 0.32 mg/L throughout the monitoring period. Iron levels initially remained very low (0.02-0.11 mg/L) during the first week, surged to a peak of 0.32 mg/L on January 30, and subsequently dropped to 0.08-0.13 mg/L by early February.

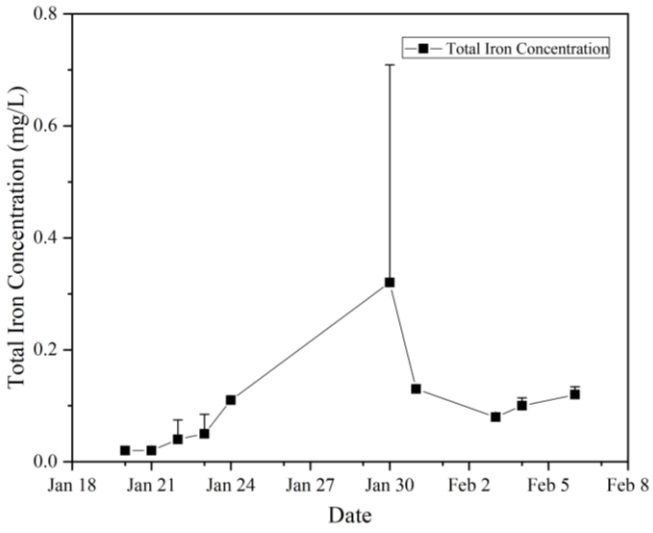


Figure 2. Fluctuation profile of total iron concentration in the MCW system

All recorded iron values remained well below the maximum quality standard threshold of < 2.0 mg/L, indicating that severe generalized corrosion was absent. Nevertheless, the peak on January 30 coincided directly with the suspension of inhibitor injection and cooling tower maintenance. These fluctuations indicate potential iron input originating from two primary sources. First, because Keramasan Combined-Cycle Power Plant utilizes surface water from the Keramasan River as raw water makeup, dissolved iron can enter the circuit through natural geological background, soil runoff, and anthropogenic contamination upstream. Surface river water is inherently vulnerable to dynamic environmental changes, causing natural variations in mineral and heavy metal concentrations (Velda et al., 2023). Second, dissolved iron (Fe^{2+}) and (Fe^{3+}) is introduced through the continuous electrochemical dissolution of carbon steel piping and structural components within the cooling circuit (Nugroho, 2015). To quantitatively distinguish between raw water iron

 https://doi.org/10.68712/zpvssq65

influx and internal piping corrosion, a mass-balance approach based on the system's Cycles of Concentration (CoC) can be applied (Rahmani, 2017). The theoretical baseline iron concentration contributed solely by the make-up water is expressed as $[Fe]_{baseline} = [Fe]_{make\text{-}up} \times CoC$. An observed concentration in the MCW loop exceeding this theoretical baseline ($[Fe]_{MCW} > [Fe]_{baseline}$) provides a direct quantitative measure of active internal metallic dissolution (Rahmani, 2017). Operational evidence in this study confirms that internal pipe corrosion was predominant driver of the observed iron peak. On January 30, the sharp iron spike (0.32 ± 0.389 mg/L) occurred concurrently with the temporary cessation of corrosion inhibitor injection during condenser maintenance. This temporal alignment strongly indicates that internal electrochemical dissolution of the carbon steel piping was the primary source of the elevated iron levels during that specific period, rather than raw river water fluctuation. In an open-recirculating cooling system, the speciation and stability of iron species are strongly governed by environmental parameters, including water pH, bulk temperature, dissolved oxygen levels, and the presence of corrosion inhibitors (Atmadja, 2010).

In localized acidic microenvironments, elevated hydronium ion (H^+) concentrations accelerate the cathodic reaction, driving the oxidative dissolution of metallic iron into soluble ferrous ions (Fe^{2+}), In the presence of dissolved oxygen within the aerated cooling tower water, the cathodic reduction of oxygen generates hydroxide ions. The combination of ferrous and hydroxide ions forms insoluble ferrous hydroxide precipitate. Ferrous hydroxide is thermodynamically unstable under oxygenated conditions and undergoes rapid secondary oxidation by water and dissolved oxygen to yield ferric hydroxide. Ferric hydroxide subsequently dehydrates and transforms into hydrated ferric oxide, commonly recognized as rust residues:

$$Fe_{(s)} \rightarrow Fe^{2+}{}_{(aq)} + 2e^-$$
$$H_2O_{(l)} + \frac{1}{2}O_{2(g)} + 2e^- \rightarrow 2OH^-{}_{(aq)}$$
$$Fe_{(s)} + H_2O_{(l)} + \frac{1}{2}O_2 \rightarrow Fe(OH)_{2(s)}$$

This transformation indicates that active corrosion on pipe walls and metal fittings serves as an internal contributor to iron presence in the cooling loop. Therefore, comprehensive baseline iron monitoring in the upstream raw water intake is essential to differentiate between background river water ingress and internal system degradation. If elevated iron levels are detected at the raw water intake, pre-treatment optimization (such as enhanced coagulation and filtration) must be prioritized prior to cooling circuit introduction. Conversely, if iron elevation occurs predominantly inside the recirculating loop, chemical corrosion inhibition strategies and regular mechanical maintenance must be intensified to suppress metallic iron release and maintain equipment integrity.

4. Conclusion

Chemical analysis of the Main Cooling Water (MCW) at Keramasan Combined-Cycle Power Plant revealed that phosphate (PO_4^{3-}) concentrations ranged from 0.28 to 2.82 mg/L, consistently failing to meet the plant operational standard of 6.0-11.0 mg/L. This depletion was exacerbated by the temporary suspension of corrosion inhibitor injection and system blowdown during maintenance. In contrast, total iron (Fe) concentrations ranged between 0.02 and 0.32 mg/L, which remained well within the safe operational threshold of < 2.0 mg/L. To optimize cooling water performance and prevent long-term corrosion degradation, it is recommended to recalibrate the corrosion inhibitor injection dosing and implement periodic iron monitoring on the Keramasan River raw water source.

Acknowledgement

The authors express their gratitude to PT PLN Indonesia Power UBP Keramasan, particularly and the laboratory team, for their technical assistance and facility access. Gratitude is also extended to the Department of Chemistry, UIN Raden Fatah Palembang, especially Ms. Ade Oktasari, M.Sc., for the guidance and support.

References

Anjarsari, N., & Sugiarso, R. D. (2019). Analisa Gangguan Ion Merkuri(II) Terhadap Kompleks Besi(II)-Fenantrolin Menggunakan Metode Spektrofotometri UV-Vis. *Jurnal Sains Dan Seni ITS*, *4*(2), 139–142. https://doi.org/10.12962/j23373520.v4i2.14027

Aprilia, D., & Hardjono. (2021). Penentuan Efisiensi Boiler Dengan Menggunakan Metode Langsung di PT X Lumajang. *DISTILAT: Jurnal Teknologi Separasi*, *7*(2), 421–426. https://doi.org/10.33795/distilat.v7i2.237

Atmadja, S. T. (2010). Pengendalian Korosi Pada Sistem Pendingin Menggunakan Penambahan Zat Inhibitor. *Rotasi*, *12*(2), 7–13.

Bastidas, D. M., Martin, U., Bastidas, J. M., & Ress, J. (2021). Corrosion inhibition mechanism of steel reinforcements in mortar using soluble phosphates: A critical review. *Materials*, *14*(20). https://doi.org/10.3390/ma14206168

Demadis, K. D., & Ketsetzi, A. (2007). Degradation of phosphonate-based scale inhibitor additives in the presence of oxidizing biocides: "Collateral damages" in industrial water systems. *Separation Science and Technology*, *42*(7), 1639–1649. https://doi.org/10.1080/01496390701290532

Dharma, I. A. (2018). *Thermal Design CCCW Heat Exchanger PLTU Dengan Variasi Kecepatan Sisi Pipa dan Baffle Spacing Menggunakan Software dan Analisis Termodinamika dan Perpindahan Panas* [Thesis, Institut Teknologi Sepuluh Nopember]. http://repository.its.ac.id/id/eprint/57366

Fakhry, M. R. N., Syuriadi, A., & Wijayanti, F. (2024). Analisa Kebutuhan Make Up Water Cooling Tower Pada PLTU 150 MW. *Prosiding A Seminar Nasional Teknik Mesin Politeknik Negeri Jakarta*, 890–896. http://prosiding.pnj.ac.id

Muammar, Fauzan, & Zamzami. (2022). Studi Proses Cooling Sistem Pada Pembangkit Listrik Tenaga Mesin Gas di PT. PJB Ubjom Pltmg Arun. *Journal Tektro*, (2), 245–250. https://doi.org/10.30811/tektro.v6i2.3739

Nugroho, F. (2015). Penggunaan Inhibitor Untuk Meningkatkan Ketahanan Korosi Pada Baja Karbon Rendah. *Jurnal Angkasa*, *7*(1), 151–158.

Rahmani, K. (2017). Reducing water consumption by increasing the cycles of concentration and Considerations of corrosion and scaling in a cooling system. *Applied Thermal Engineering*, *114*, 849–856. https://doi.org/10.1016/j.applthermaleng.2016.12.075

Rahmawati, A. U., Wikendi, L., Maryanty, Y., & Yusuf, N. K. (2024). Analisis Proses Kimia Dalam Siklus Uap Air di PLTU Paiton Unit 1 dan 2. *DISTILAT: Jurnal Teknologi Separasi*, *10*(3), 562–571. https://doi.org/10.33795/distilat.v10i3.6238

Rayadi, I. T. (2015). Pemanfaatan Air di Industri Perminyakan. In *Bisnis Air di Bidang Perminyakan*. https://www.researchgate.net/publication/287595684_Pemanfaatan_Air_di_Industri_Perminyakan

Syafika, N., Novita, N., Masrura, M., & Amalia, N. F. (2022). Pengaruh Konsentrasi Nitrit Dan Molybdate Sebagai Corrosion Inhibitor Terhadap Konsentrasi Besi (Fe) Pada Air Pendingin di PT Perta Arun Gas. *Amina*, *4*(3). https://doi.org/10.22373/amina.v4i3.553612

Velda, N. A., Wardhani, E., & Wulan, D. R. (2023). Studi Pustaka: Kontaminasi Logam Berat Terlarut pada Air Sungai. *FTSP Series : Seminar Nasional Dan Diseminasi Tugas Akhir*, 2154–2159.